Decay Characteristics of Surface Mounds with Contrasting Interlayer Mass Transport Channels

Maozhi Li,[1] J. F. Wendelken,[2] Bang-Gui Liu,[1] E. G. Wang,[1] and Zhenyu Zhang[2]

[1]*Institute of Physics & Center of Condensed Matter Physics, Chinese Academy of Sciences, P.O. Box 603, Beijing 100080, People's Republic of China*

[2]*Solid State Division, Oak Ridge National Laboratory, Oak Ridge, Tennessee 37831-6032*

(Received 16 October 2000)

The decay characteristics of three-dimensional (3D) islands formed on surfaces are investigated theoretically considering two types of interlayer mass transport mechanisms. If an adatom on a given layer can easily descend from any site along the periphery of the layer, an optimal island slope and a constant terrace width will be selected during the decay. In contrast, if the adatom can descend primarily through selective (such as kinked) sites, the decay will be accompanied by a gradual increase in the island slope. These generic conclusions provide the basis for a microscopic understanding of the decay of nanostructures in fcc(111) and fcc(100) metal homoepitaxy and are applicable to other systems as well.

DOI: 10.1103/PhysRevLett.86.2345 PACS numbers: 61.43.Bn, 68.37.Ef, 68.55.–a, 68.60.Dv

Understanding the mechanisms and kinetics involved in the formation and stability of nanostructures on surfaces is of vital importance for the fast-growing area of nanotechnology. In recent years, much progress has been made in elucidating the atomic-scale mechanisms and morphological evolution during the growth of thin films and various nanostructures such as three-dimensional (3D) islands (quantum dots or mounds) [1,2]. In contrast, much less effort has been devoted to the stability of such low-dimensional structures after their formation [3], although understanding their stability is a prerequisite for potential device applications.

For formation by atom deposition, it is well recognized that the Ehrlich-Schwoebel (ES) barrier [4,5], an additional potential energy barrier against the descent of atoms at step edges, primarily controls interlayer mass transport and may result in the formation of quantum dots (QDs) or mounds. Once formed, how atoms descend from one layer to a lower layer is expected to be a key process in controlling the stability or decay of the QDs. Recent studies have shown that the ES barrier can be quite different for different systems. For a given system, it can also vary significantly with the orientation of the surface [6–10], be influenced by step meandering (kinked steps), and depend on the size of the layer. Recent experimental studies have further shown that interlayer mass transport may proceed as an avalanche due to fast transfer of atoms via edge diffusion to an effective descent channel [11]. Qualitatively, it is tempting to associate faster interlayer mass transport with less stable mounds, but precisely how these vastly different descent mechanisms influence the decay of the mounds remains an intriguing question.

In this Letter, we investigate how the two most common types of atom descent mechanisms influence the stability and decay of 3D nanostructures on surfaces. The first is when an atop atom can easily descend from any edge site (the ASD, or any-site descent mechanism). The other is when an atop atom has to descend primarily through some selective (such as kinked) sites (the SSD, or selective-site descent mechanism). We first show theoretically that these two different interlayer mass transport mechanisms will have distinctly different signatures in the decay characteristics of the 3D islands. If the islands decay primarily via the ASD mechanism, an optimal island slope and a constant terrace width will be selected. In contrast, for the SSD mechanism, the island decay will be accompanied by a gradual increase in the island slope. These generic conclusions provide the basis for a microscopic understanding of the morphological evolution observed in existing experimental studies of island smoothening for a variety of systems, as well as the decay of 3D Cu islands on the (100) and (111) surfaces of Cu observed in the present study.

Our theoretical studies of island decay are carried out by kinetic Monte Carlo simulations. In these simulations, we construct as the initial state a 3D island of varying heights and layer areas on an ideally flat surface modeled by a square lattice, and we define an active zone much larger than the area of the bottom layer. If an adatom diffuses out of this active zone during the island decay, it is more likely to join some other surface defects (such as preexisting steps and islands) than returning to the original island; therefore, it can be removed from the system. Three elemental kinetic processes are important in island decay: atom detachment from the periphery of a layer, diffusion across the terrace, and descent at the step edge, described by activation energies V_d, V_t, and V_s, respectively. The corresponding rate is represented by $R_i = \nu \exp(-V_i/k_BT)$, where V_i is the activation energy for process i, k_B is the Boltzmann constant, and T is the temperature. The attempt frequency is chosen as $\nu = k_BT/h = 4.1671 \times 10^{10}T$, with h Planck's constant, and T given in degrees Kelvin.

We first study island decay primarily via the ASD mechanism. Here we start with a seven-layer island containing about 13 000 atoms. Each terrace width between the edges of two adjacent layers is set to be five atoms wide in the close-packed direction. The energy parameters used in the simulations are shown in Fig. 1, including $V_d = 0.65$ eV, $V_t = 0.35$ eV, and $V_s = 0.43$ eV

[7–9]. The barrier for atom descent at kinked sites, $V_{sk} = 0.40$ eV, is only slightly lower than the barrier V_s, ensuring that the ASD mechanism is the dominant one.

The layer-resolved evolution of the island at 400 K is shown in Fig. 2(a), with 1 through 7 denoting the top through the bottom layer, respectively. Within the ASD mechanism, the most distinctive feature of the island decay is that the total number of atoms in each layer decreases approximately linearly, and with an equal rate. Therefore, as the island shrinks, the different layers maintain a roughly constant slope as defined for the initial island. This feature is also evident in Fig. 3(a) where Ti ($i = 1, 2, 3, 4, 5, 6$) denotes the terrace width between layer i and layer $i + 1$. Except for T1, the remaining terraces essentially maintain equal widths during the decay as indicated by the plots of Ti and the two snapshots depicting the initial configuration and that after 100 s. For T1, because no atom is added onto the first layer whereas atoms are continuously descending to the lower layer, T1 is monotonically increasing and can no longer be defined once the top layer disappears.

In order to examine how strongly a constant slope is preferred, we have also simulated the evolution of an island whose initial state contains very different terrace widths. The results are shown in Fig. 3(b). Here the narrower terraces become broader, and the broader terraces become narrower, eventually reaching a constant and optimal slope for the lower layers. This constant slope is maintained until the highest layer of this subgroup becomes the top layer of the whole system.

Why do the broader terraces shrink whereas the narrower terraces become wider in island decay via the ASD mechanism? This can be understood by considering the frequency with which adatoms on a given terrace visit the outer step edge surrounding the terrace. With identical activation energy parameters, the more frequently an adatom reaches the outer edge, the more quickly it will descend to a lower terrace. The visit frequency scales inversely with the terrace width [12]. Therefore, an adatom detached from a layer surrounded by a narrower terrace is more likely to descend quickly to a lower layer than to return to the same layer, thereby increasing the terrace width. Similarly, a broader terrace will shrink its width due to a fast supply of adatoms from its upper layer with a narrower terrace and slow escape of adatoms to a lower terrace. Once the terrace widths are equalized, a steady state with an optimal slope and the constant terrace width will be maintained.

We next study island decay primarily via the SSD mechanism. Similarly, we start with a five-layer island containing about 6000 atoms. Each terrace width is set to be five atoms wide again. The energy parameters used in the simulations are shown in Fig. 1, which are close to the known results for Cu(100) [7–9]. Here $V_d = 0.8$ eV, $V_t = 0.43$ eV, and $V_s = 0.62$ eV. Furthermore, $V_{sk} = 0.52$ eV is significantly lower than V_s, ensuring that the SSD mechanism is dominant. The layer-resolved evolution of the island at 400 K within the SSD mechanism is shown in Fig. 2(b). Here the behavior is distinctly different from that shown in Fig. 2(a) for the ASD case. Most notably, the middle layers exhibit very weak time dependence, despite the fact that the overall size of the island is shrinking. The decay rate is largest for the bottom and top layers (layers 5 and 1). Therefore, as the island decays, the constant slope of the initial island becomes steeper on average. This feature is qualitatively attributable to the fact that under the SSD mechanism, atoms can effectively detach and diffuse away from the island and out of the active zone, whereas atoms detached from the upper layers cannot find enough channels to effectively descend to the lower layers. It should be noted that, in practice, the slope increase will cease when it reaches a certain value corresponding, for example, to a facet orientation of a given physical system. At such an angle, the system is energetically more stable, making further decay of the faceted island more difficult.

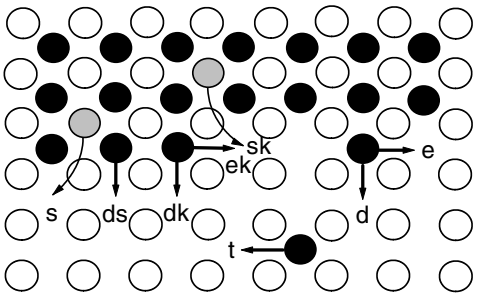

	t	s	sk	e	ek	d	dk	ds
ASD	0.35	0.43	0.40	0.40	0.50	0.65	0.65	1.00
SSD	0.43	0.62	0.52	0.30	0.51	0.80	0.80	1.00

FIG. 1. Various diffusion processes and the corresponding energy barriers (in units of eV) involved in the ASD and SSD mechanisms, as illustrated on a fcc(100) surface. The white, black, and gray circles denote atoms in the lower, the middle, and the upper layer, respectively.

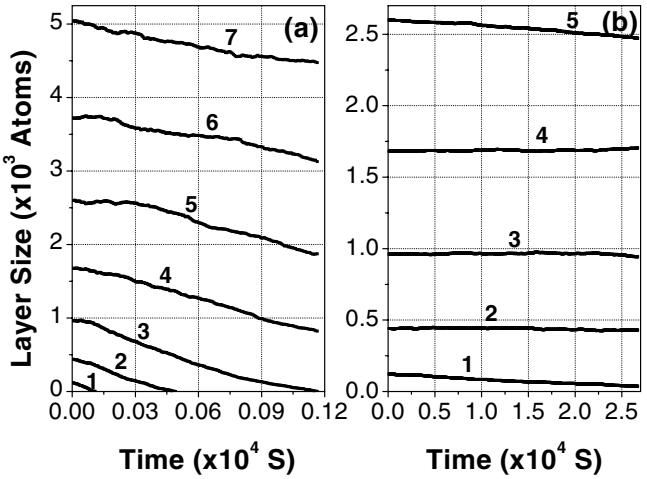

FIG. 2. The layer-resolved evolution of an island decaying at 400 K (a) via the ASD mechanism and (b) via the SSD mechanism.

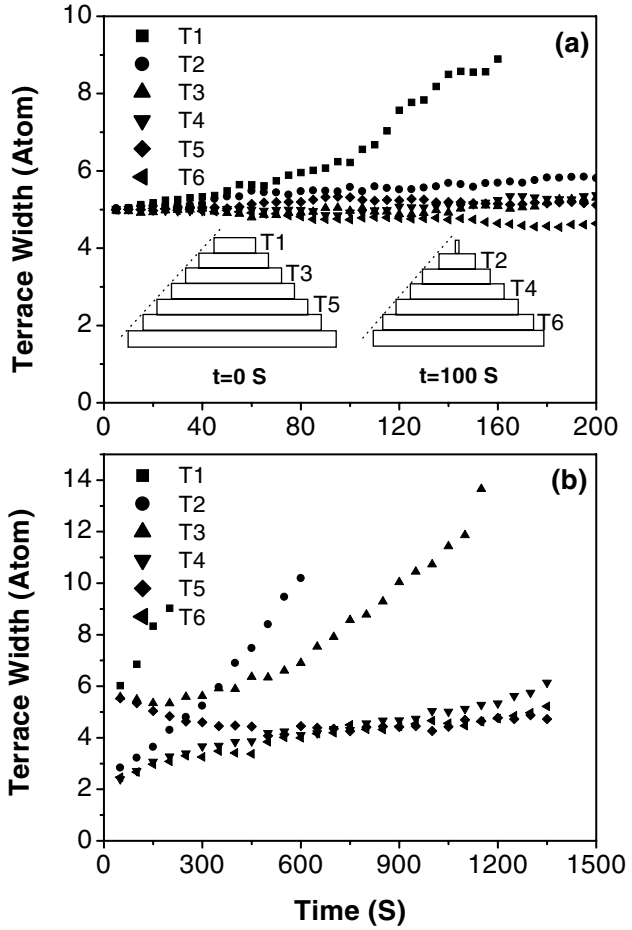

FIG. 3. The evolution of terrace width with time at 400 K under the ASD mechanism for (a) initially equal terrace widths and (b) initially unequal terrace widths.

For a given system, if the absolute magnitude of V_s is small, the system is more likely to obey the ASD mechanism, because an adatom reaching a straight segment of the step edge has no need to search for a more effective kink site to descend. If, instead, V_s is large, then the island decay is more likely to obey the SSD mechanism, because an adatom reaching the step edge will have to attempt many times before finding a kink site and making a successful descent. Based on these considerations, we anticipate that island decay on the fcc(111) metal surfaces will obey the ASD mechanism, because it is known that the absolute magnitude of V_s is small in such systems. In contrast, islands formed on the fcc(100) surfaces are more likely to obey the SSD mechanism, because of the relatively large magnitudes of V_s in such systems. Another influential factor is that the reduction in V_s by the presence of a kinked site is more effective on the open surfaces of fcc(100) than that on the closely packed fcc(111) surfaces. It is worth noting that in epitaxial growth it is the ES barrier, $V_{\mathrm{ES}} = V_s - V_t$, which dictates the roughness of the growth front; whereas in island decay, it is the absolute magnitude of V_s which has a crucial influence on the decay characteristics.

Indeed, in existing experimental studies of island formation and decay, it has been observed that the islands can select an optimal slope and a unique terrace width on the fcc(111) metal surfaces. Examples include the decay of Ag clusters deposited on Ag(111) surfaces [13]. As the nearly hemispherical islands decay on the surfaces, they reach a common steady state with an optimal slope and a sharp terrace width distribution. Another beautiful example is provided in the formation of stair-stepped Pt islands on Pt(111) [14]. In contrast, to the best of our knowledge no such islands have ever been observed on fcc(100) surfaces. Instead, 3D islands with well-defined facets have been observed in several fcc(100) systems, for example, in the case of Cu(100) homoepitaxy [15].

In order to compare more directly between theory and experiment, we have performed layer-resolved investigation of the decay of 3D Cu islands on the Cu(100) and Cu(111) surfaces. The most striking comparison of these two surfaces was obtained by making movies of the decay process at a temperature of 297 K using a scanning tunneling microscope (STM). The Cu(100) data were obtained after deposition of 140 ML (monolayer) of Cu and the Cu(111) data were obtained after deposition of 5 ML. The smaller deposition on Cu(111) was used since 3D islands develop more rapidly on the Cu(111) surfaces.

We note that the experimental data were obtained at room temperature, i.e., 297 K, whereas the simulation results were obtained at 400 K. As is described below, this difference in temperature results in different diffusion mechanisms via which atoms are supplied to the island edges. Nevertheless, the salient features predicted in the simulation results within the ASD and the SSD mechanisms are still apparent in the experimental data, showing the dominance of the atom descent mechanism.

In our simulations at 400 K, atoms readily evaporate from edges and then diffuse across the terraces. This is already apparent in the work of Hannon *et al.* [16] where the evaporation condensation mechanism provides the major mechanism for monolayer island coarsening on Cu(100) at 343 K. In contrast, for the same system, but at 297 K, Pai *et al.* [17] found that evaporation from edges is an insignificant factor in the mass flow on the surface in which monolayer islands are found to diffuse by perimeter diffusion. Consistent with these earlier observations [11,17], here we find on both Cu(100) and Cu(111) surfaces that the most rapid decay of the top layer of a 3D island occurs when the edge of the top layer comes in contact with the edge of the next layer down. Atoms are supplied readily to the edge via edge diffusion resulting in a fast decay process which may be referred to as an avalanche. The key difference, however, lies on the rate of atom descent on the contact angle. For Cu(111), we find, as in Ref. [11], that there is no dependence on the site where the point of contact occurs; i.e., the barriers for the avalanche process at all edges are the same. In contrast, for Cu(100), if the top layer moves in contact with the straight edge of the layer below, nothing happens. Only when the layer moves

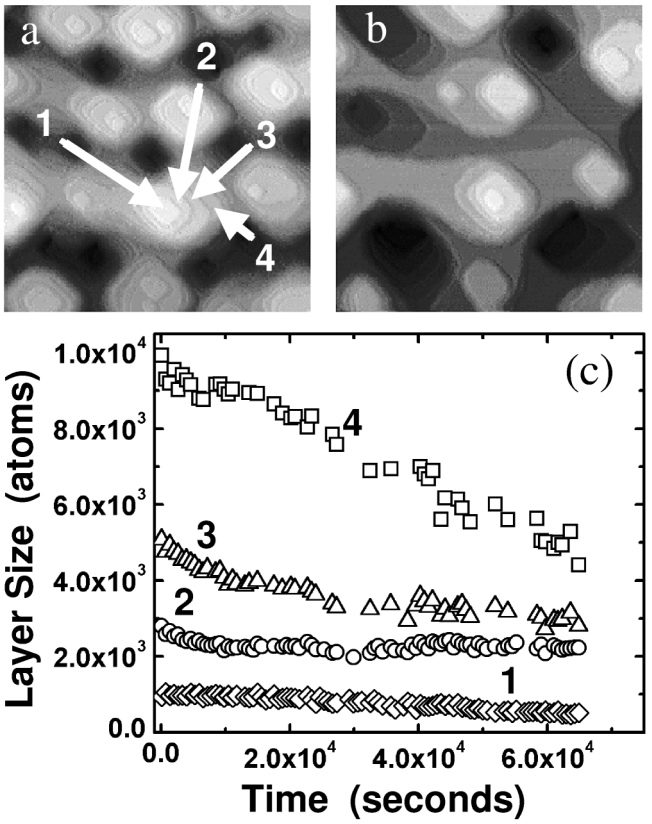

FIG. 4. Experimental measurement of mound decay on Cu(100) vs time at 297 K. (a) STM image after deposition of 140 ML with four layers of selected mounds indicated, (b) the same mound six hours later, and (c) the measured areas of the four layers vs time. The image sizes are 100×100 nm^2.

in contact with a corner is a rapid decay in the layer size observed. Thus on the Cu(100) surface, we have a site-dependent avalanche process.

Figure 4 shows the experimental results obtained for the decay of a single 3D Cu island on the (100) surface at 297 K. The initial state of the surface is shown in Fig. 4(a) and the condition after six hours is shown in Fig. 4(b). The selected island consists of four layers on top of a midlevel terrace that separates the islands from roughly symmetric holes. As shown in Fig. 4(c), the bottom layer decays with the fastest rate, whereas the top layer decays with the slowest rate, leading to a steeper slope of the island sides as it decays. This qualitative feature illustrated for the selected island is in fact valid generally, based on our observation on the behavior of many such islands on Cu(100). In contrast, we find that the decay of Cu islands formed on Cu(111) is characterized by the selection of an optimal slope and roughly equal terrace widths, which is similar to the case of Ag islands on Ag(111) [13]. As expected from the model predictions, the decay characteristics are signatures of the dependence of the avalanche process on the contrasting descent mechanisms. It can take place at any contact angle on Cu(111), resembling the ASD mechanism; but only at certain corner sites on Cu(100), resembling the SSD mechanism.

In summary, we have shown that the two most common types of atom descent mechanisms at step edges, the any-site and the selective-site descent mechanisms, will lead to distinctly different characteristics in the stability and decay of 3D islands on surfaces. If the islands decay primarily via the ASD mechanism, an optimal island slope and a constant terrace width will be selected. In contrast, within the SSD mechanism, the island decay will be accompanied by a gradual increase in the island slope and the likely formation of facets. These generic conclusions provide the basis for a microscopic understanding of the morphological evolution observed in both the existing and the present experimental studies of island formation and smoothening on the fcc(111) and fcc(100) metal surfaces and should be applicable to other systems as well.

This work was partly supported by the Natural Science Foundation of China, by the China National Key Projects on Basic Research, and by Oak Ridge National Laboratory, managed by UT-Battell, LLC, for the U.S. Department of Energy under Contract No. DE-AC05-00OR22725.

[1] Z. Y. Zhang and M. G. Lagally, Science **276**, 377 (1997).
[2] F. J. Himpsel, J. E. Ortega, G. J. Mankey, and R. F. Willis, Adv. Phys. **47**, 511 (1998).
[3] For a few examples, see J.-K. Zuo and J. F. Wendelken, Phys. Rev. Lett. **78**, 2791 (1997); N. Israeli and D. Kandel, *ibid.* **80**, 3300 (1998); A. Ichimiya *et al., ibid.* **84**, 3662 (2000).
[4] G. Ehrlich and F. G. Hudda, J. Chem. Phys. **44**, 1039 (1966).
[5] R. L. Schwoebel and E. J. Shipsey, J. Appl. Phys. **37**, 3682 (1966).
[6] B. D. Yu and M. Scheffler, Phys. Rev. Lett. **77**, 1095 (1996).
[7] M. Karimi, T. Tomkowski, G. Vidali, and O. Biham, Phys. Rev. B **52**, 5364 (1995).
[8] O. S. Trushin *et al.,* Phys. Rev. B **56**, 12 135 (1997).
[9] H. Mehl, O. Biham, I. Furman, and M. Karimi, Phys. Rev. B **60**, 2106 (1999).
[10] M. I. Haftel and T. L. Einstein, in *Nucleation and Growth Processes in Materials,* edited by A. Gonis, P. E. A. Turchi, and A. J. Ardell, MRS Symposia Proceedings No. 580 (Materials Research Society, Boston, 1999), p. 195.
[11] M. Giesen, G. Schulze Icking-Konert, and H. Ibach, Phys. Rev. Lett. **80**, 552 (1998).
[12] G. Rosenfeld *et al.,* Phys. Rev. Lett. **71**, 895 (1993).
[13] S. J. Chey, L. Huang, and J. H. Weaver, Surf. Sci. **419**, L100 (1998).
[14] J. Krug, P. Politi, and T. Michely, Phys. Rev. B **61**, 14 037 (2000).
[15] H.-J. Ernst, F. Fabre, and J. Lapujoulade, Phys. Rev. Lett. **69**, 458 (1992).
[16] J. B. Hannon *et al.,* Phys. Rev. Lett. **79**, 2506 (1997).
[17] Woei Wu Pai, Anna K. Swan, Zhenyu Zhang, and J. F. Wendelken, Phys. Rev. Lett. **79**, 3210 (1997).